Fabrication of functionalised surfaces on Gum metal (Ti-30Nb) using micromachining

Sara Hawi[1], Andrew Dickins[1], Goncalo Rodrigues Pardal[1], Claudiu Giusca[1], Oliver Pearce[2], Saurav Goel[1‡]

[1] School of Aerospace, Transport and Manufacturing, Cranfield University, Cranfield, MK43 0AL, UK
[2] Milton Keynes Uni hospital, Standing Way, Eagelstone, MK65LD, Milton Keynes, UK

‡S.Goel@cranfield.ac.uk

Abstract

Structured surfaces are attracting deep interest, as they allow tailoring the functionality via changes in the surface topography. Applications for these surfaces range greatly, including, optical surfaces for antireflective surfaces, thermal structures to assist in heat dispersion and anti-fouling surfaces to reduce micro-organisms from adhering to components. Gum metal is a relatively newer kind of beta titanium alloy that has earmarked its place as the next generation Ortheopedic implant material. In a timely effort, this work investigated the generation of micron level structured surfaces on Gum metal (Ti-30Nb – a beta titanium alloy) to explore micromilling as the robust scalable process to achieve low dimensional surfaces in titanium alloy. During micromilling, the feedrate, spindle speed, axial depth of cut and tool step over were varied to optimise these parameters for achieving superior quality of machining.

Keywords:
Gum metal, surface functionalisation, micromachining, Taguchi matrix

1. Introduction

Nature has long inspired advancement in science and technology. Nature inspired structured surfaces gained popularity during the 1990s and are continuously being investigated for a better understanding of their functionalities such as controlled wettability, bactericidal activity and optical reflectivity [1][2].

It is a common understanding that these functional properties are dictated by surface topography, surface energy and material's microstructure. To date, surface structuring has been primarily achieved by using laser texturing, contact mode machining, chemical etching and coating techniques. Literature suggests that the materials of choice for the manufacturing of micro/- or nano/- structured surfaces have been limited to polymers, steels and brass.

Titanium alloys are extensively used both in aerospace and biomedical sectors and have attracted a great deal of manufacturing research for being classed as "notoriously difficult to cut materials" [3]. It is plausible that this difficulty is the reason that literature concerning surface functionalisation of titanium alloys especially using micro-milling is rather scarce. This work aims to demonstrate a manufacturing strategy for observing wetting behaviour of gum metal (Ti-30Nb – a beta titanium alloy) using the process of micromilling. An improved understanding of the optimal machining parameters, conditions and inspection of the machined surface would be beneficial in the fabrication of many materials used in other engineering domains.

2. Background

Wettability is commonly estimated by contact angle measurements, where a droplet is placed onto a sample and the angle between the liquid-atmosphere interface and the liquid-surface interface is measured. In general, a contact angle (CA) of less than 90° is defined as a hydrophilic response, and a contact angle larger than 90° seems to suggest hydrophobic behaviour. A great inspiration of controlled wettability stems from the self cleaning behaviour of many plant leaves, with the lotus leaf (CA as high as 160°) being a noteworthy example [5].
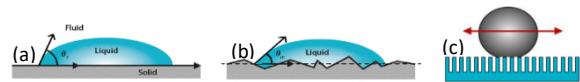

Figure 1: (a) Wetting on a smooth surface, (b) Wenzel's Wetting Model, (c) Cassie & Baxter's Wetting Model [4]

The earliest model that correlates wettability with surface topography was addressed by Wenzel [6]. This model assumes that the contour of the topography is fully wetted by the liquid and that the contact angle is dependent on the surface area of the topography. Wenzel introduced a roughness ratio (*r*) which is the actual surface area of the solid over the projected area. He established the equation for the contact angle (θ) as:

$$\cos \theta_w = r \cos \theta \qquad (1)$$

where θ_w is the apparent contact angle corresponding to the stable equilibrium state.

Cassie and Baxter [7], later, suggested a model in which the droplet may have contact only with the top of the topographic features. The model proposes that there are air-filled gaps in the surface which would break the contact. Thus, a new equation was established:

$$\cos \theta_c = f_1 \cos \theta - f_2 \qquad (2)$$

where θ_c is the resulting contact angle of the structured surface, f_1 and f_2 are the ratios of the contact areas between the drop and solid and the drop and air respectively.

Thus, the Cassie Baxter model suggests that surface hydrophobicity increases by structuring the surface in a way that air entraps in the grooves under the water droplet and the contact angle between the surface and the droplet is decreased.

3. Research methodology

3.1. Materials

Gum metal (Ti-30Nb) is a beta type titanium alloy that has gained light recently and rivaled Ti-6Al-4V in biomedical applications due to its lower Young's modulus (closer to that of bone), and its less toxic alloying element, granting better biocompatibility. The tools used for machining were Tungsten Carbide endmills of 5 mm diameter for the machining of test squares and 200 µm diameters for machining of grooves. The cutting tools were bought from "Rainford Precision" who are an approved supplier of KERN Evo Micromilling machine tool used in this work.

3.2. Design of experiments

The parameters for micro-milling were chosen based around micro-milling parameters of Ti-6Al-4V found in the literature and according to a statistical method that is designed for quality optimisation of a process developed by Taguchi [8]. Three levels of input machining parameters were factored into the Taguchi experimental matrix. The input machining parameters (see table 1) that were varied are the spindle speed, feed rate, axial depth of cut and tool pass overlap as they tend to influence the surface quality during micromilling.

Table 1: Levels and factors of machining parameters used

Parameter	Level 1	Level 2	Level 3
Spindle speed (rpm)	20000	30000	40000
Feed rate (mm/min)	50	150	250
Depth of cut (µm)	5	10	15
Step over factor	1.0	1.5	1.99

3.3. Machining

Squares of 5 mm X 5 mm were made on the alloy sample. Half of each square was skimmed flat while the other half had six grooves machined into it (figure 2). Both the skimming and groove machining used the same parameters across the same square (table 1). No coolant was used during the machining.
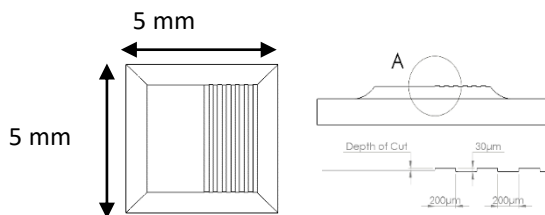

Figure 2: Drawing of the machined squares and features (a) top view (b) Side view (c) groove dimensions

3.4. Instrumentation for post-machining examination

The Dektak ST3 surface profilometer (12.5 µm radius and 60º cone angle diamond tip probe) was used to conduct 2D profile measurements across the direction of lay to measure and compare the deviations from the programmed geometries.

An environmental-Scanning Electron Microscope (eSEM) was used post machining to determine any occurence of diffusion arising from the migration of carbon atoms from the cutting tool to the titanium atoms of the workpiece. Three images were

acquired on each flat surface from three grooves on each pillar. Images of the tools post machining were acquired as well.

The wettability was evaluated by measuring the contact angle of water drops twice on each of the squares of Ti-30Nb; once on the grooved surface and once on the flat surface. Droplet sizes were kept to be of similar volumes to achieve comparable results. Images were acquired with the camera's line of sight parallel to the groove direction and also with the line of site perpendicular to the groove direction (as shown in figure 3).
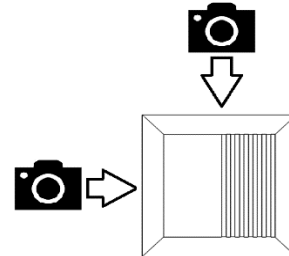

Figure 3: Directions of contact angle measurements

4. Results and Discussion

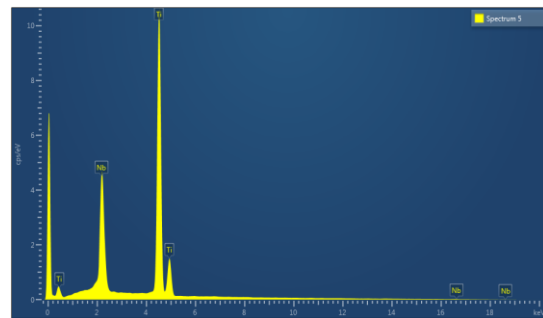### 4.1. Energy Dispersive Spectroscopy of premachined sample

Figure 4: EDS spectrum of pre-machine Ti-30Nb

Before machining trials, gum metal sample was analysed using the energy dispersive spectroscopy (EDS). Pre-machined EDS analysis of the gum metal (beta Titanium Alloy) yielded a composition of 72.60wt% of Ti and 27.40wt% of Niobium (see figure 4).

4.2. Surface profile measurements

Profiles taken across the grooves showed that the depth of groove was not exactly 30 µm as programmed. Groove depths vary from approximately 21 µm to 32 µm for different trials on the Ti-30Nb sample, with some showing a consistent depth
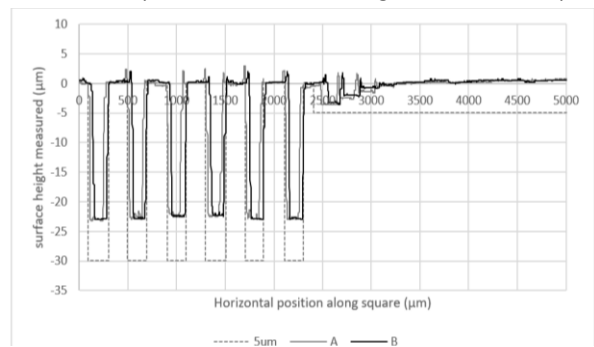

Figure 5: Form profile of Ti-30Nb square 1: DOC 5 µm, overlap 1.99, feed 50 mm/min, ss20000 rpm),. Line A is from the left of the square, line B is from the right and the dashed line represents the targeted profile.

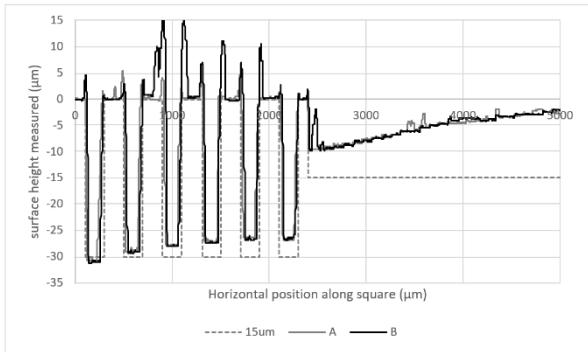across all grooves machined (Figure 5), and others varying greatly over the same square (Figure 6).

Figure 6: Form profile of Ti-30Nb square 3: DOC 15 µm, overlap 1, feed 250 mm/min, ss20000 rpm

The profiles of the flat surfaces presented a gradual decrease in depth. This deviation in machining depth was observed to be maximal when small depth of cut (5 µm) was used where only a small portion of the surface was flat (Figure 5). The measurement of the diameter of the end mill in few cases seems to be about 180 µm. This seems to be the reason that certain thin sections between the machining passes remained unmachined whilst using 1.99 step over. Figure 5 and Figure 6 are collectively emotive of certain deviations in the programmed and measured depth of grooves. A careful consideration of these deviations indicates random errors in the position axis of the machine tool as no significant wear of the tool was observed post machining that would have caused these deviations.

For estimation of the productivity during micromilling, the material removal rate (MRR) of gum metal was calculated as follows:

$$MRR = \frac{DOC \times d \times f}{60} \tag{3}$$

where DOC is the depth of cut in mm, d is the tool diameter in mm and f is the federate in mm/min.
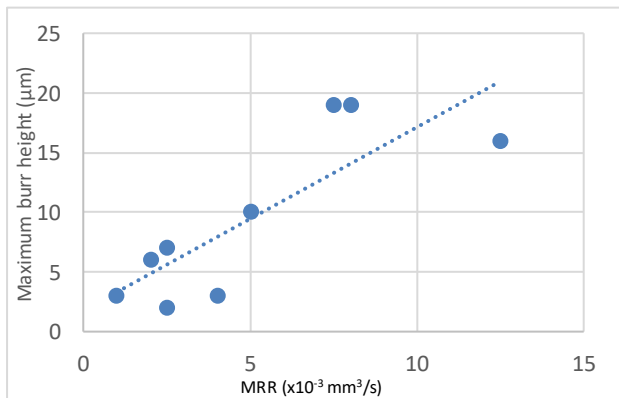

Figure 7: Maximum burr height versus material removal rate

An analysis of material removal rate against burr formation showed a direct correlation. It was noted that the burr height scales linearly with MRR (Figure 7). Thus, one could infer that a low MRR (low feed rate and depth of cut) would provide better quality structured surfaces.

However, there is a trade-off between surface quality and machining time to be taken into account when feed rate is chosen. This was demonstrated when a groove that was manufactured with a low depth of cut and low feed rate in 69 second was measured to have a lower value of Ra than a groove

that was manufactured with an intermediate depth of cut and high feed rate in 9 seconds.

4.3. Contact angle measurements

The contact angle measurements from the line of site perpendicular to the grooves' direction yielded an average of 32.81 ± 6.91° for the grooved surfaces and 24.93 ± 4.39° for flat surfaces signifying a change in the wetting conditions.

An exception to this was observed on one of the squares which recorded high burr heights during surface profile measurements.

The contact angles with line of site parallel to the grooves' direction across all squares gave a mean contact angle of 42.47 ± 19.38° for the grooved surfaces and 29.42 ± 16.82° for the flat surfaces.

The results seem to suggest an improvement in the hydrophobicity. However, when viewed from a parallel line of sight to the grooves' direction, the difference in angle was larger than 13.05°. These two observations point to the anisotropic wetting behaviour of the micromilled surface. This aspect needs further investigation and remains a follow on work.

4.4. Scanning Electron Microscopy (SEM) and elemental EDS of the machined areas

SEM imaging was done post-machining that revealed the machining-induced debris present along the grooves of the surfaces. Some regions showed more debris deposition than the other regions. EDS mapping was performed across the areas where burrs and debris were abundant. EDS images in figure 8 showed rich presence of carbon and oxygen atoms especially in built-up edges and burrs. This chemical analysis points to the presence of intermetallics involving presence of carbon compounds formed during micromilling process.
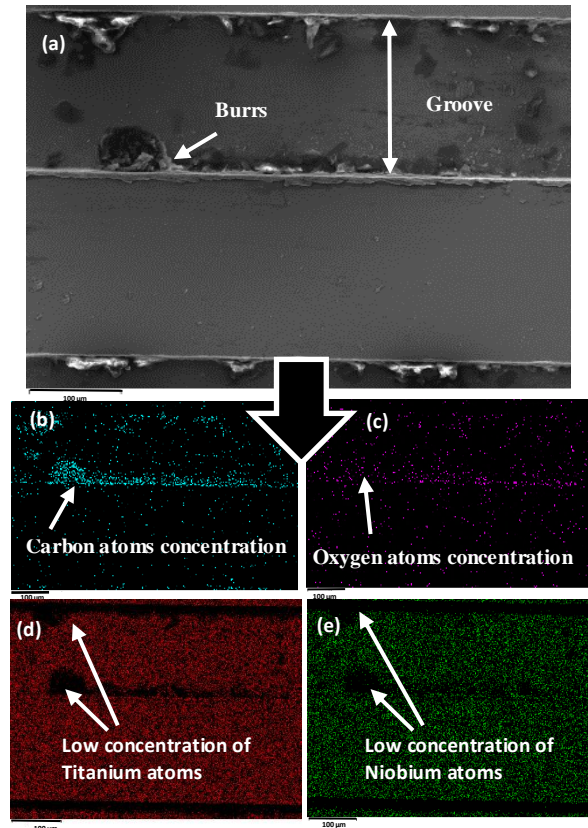

Figure 8: (a) SEM image of groove on square 7 of Ti-30Nb (b) EDS mapping data showing elemental distribution of Carbon, (c) Oxygen, (d) Titanium, (e) Niobium

4.5. Scanning Electron Microscopy (SEM) of cutting tools and debris

SEM images of the cutting tools revealed that the Tungsten Carbide end mills had minimal visible wear with no clear decrease in size or change in geometry before and after machining in any case for the length of machining performed.
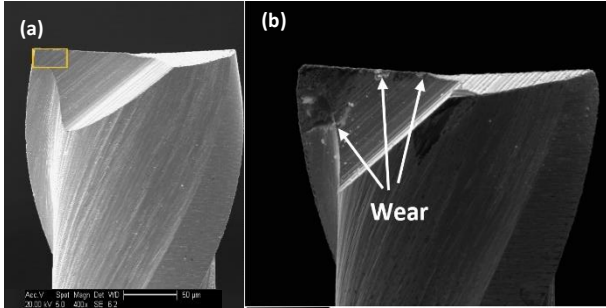

Figure 9: (a) Cutting tool before machining (b) cutting tool after machining

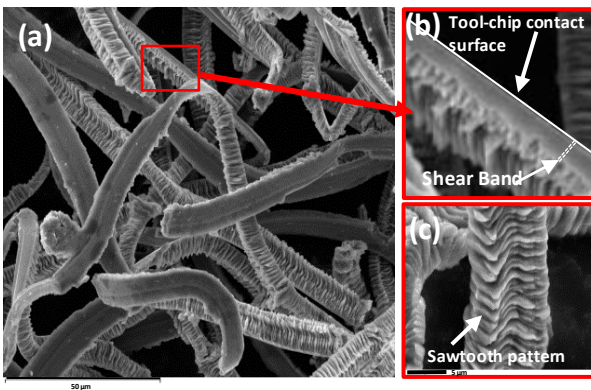However, some indications of incipient wear were identified in figure 9 (b).

Figure 10: (a) SEM image of cutting chips, (b) Magnification of chip showing shear bands, (c) Sawtooth pattern magnified

Cutting chips are fingerprint of a machining operation and therefore, they were collected and analysed in an SEM. The cutting chips shown in figure 10 were of continuous type but serrated. Literature concerning cutting chips suggest that this could be related to the effect of shear band deformation (notable in other titanium alloys).

As the cutting speed increases, the shear angle increases thus the chips are segmented by fully developed shear bands (figure 11) as explained in details by Ye *et al.* [9].
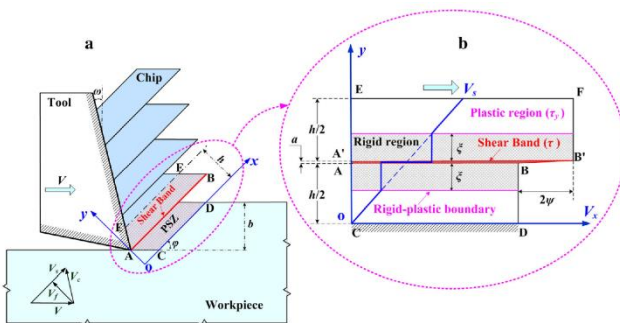

Figure 11: (a) Serrated chip flow model (b) shear band evolution model Reprinted with permission from [9], Copyright 2010 Springer

Our observation of cutting chips seems to suggest a similar phenomena occurring also in Gum metal in which case, the following equation can be used to describe the relationship of unloading stress inside the shear band.

$$\tau(t) = \tau_y(1 - X(t)) \tag{4}$$

where *t* is the evolution time of the shear band, τ_y is the initial yield stress within the plastic region, $X(t)$ is the degree of evolution of the shear band which can be described as:

$$X(t) = \frac{\varphi(t)}{\varphi_c}, 0 \leq X(t) \leq 1 \tag{5}$$

where φ_c is the critical shear displacement at which the shear band stress vanishes and the shear band is fully matured. Thus, when X(t) reaches 1, the cutting chips' flow becomes segmented.

5. Conclusion

Micro-grooves were fabricated on a Gum metal alloy (Ti-30Nb) using micro-milling with varied cutting parameters implemented *via* an experimental design approach proposed by Taguchi. The machining quality in relation to machining parameters and the wettability of the surfaces were investigated. Overall, gum metal seems to be machinable by the use of commercially available carbide tooling. The analysis of results showed that for an optimum surface finish of Ti-30Nb, there lies an optimum material removal rate that helps achieving more deterministic level of finishing (low feed rate and low depth of cut), although it comes at an expense of large machining times. In common with other class of titanium alloys, Gum metal showed serrated continuous chip with a marked presence of shear band formation.

References
[1] M. Callies, D. Quere. Soft Matter. 2005; **1**(1), 55-61.
[2] Yamada, N., Kim, O. N., Tokimitsu, T., Nakai, Y., Masuda, H. Prog. Photovoltaics 2011; **19**, 134–140.
[3] Shokrani A., Dhokia V., Newman ST. Machining Science and Technology. Taylor & Francis; 2016; **20**(3): 475–494.
[4] Attension TN 7. 2015, 1–3.
[5] Bico, J., Marzolin, C., & Quere, D. Europhysics Letters; 1999; **47**(2), 220-226.
[6] Wenzel, R. (1936). Industrial & Engineering Chemistry, **28**(8), 988-994.
[7] Cassie, B.D., Baxter, S. Trans. Faraday Soc. 1944; (5): 546–551.
[8] Rashid W Bin., Goel S., Davim JP., Joshi SN. The International Journal of Advanced Manufacturing Technology; 2016; **82**(1–4), 451–462.
[9] Ye GG., Xue SF., Ma W., Dai LH. International Journal of Advanced Manufacturing Technology. 2017; **88(**1–4): 1161–1174.

2019-06-30

Fabrication of functionalised surfaces on gum metal (Ti-30Nb) using micromachining

Hawi, Sara

euspen